



Imaging of Reactive Astroglialosis by Positron Emission Tomography

Ryuichi Harada^{1*}, Shozo Furumoto², Yukitsuka Kudo³, Kazuhiko Yanai¹, Victor L. Villemagne^{4,5} and Nobuyuki Okamura^{6*}

¹ Department of Pharmacology, Tohoku University Graduate School of Medicine, Sendai, Japan, ² Cyclotron and Radioisotope Center, Tohoku University, Sendai, Japan, ³ Department of New Therapeutics Innovation for Alzheimer's and Dementia, Institute of Development and Aging, Tohoku University, Sendai, Japan, ⁴ Department of Molecular Imaging and Therapy, Austin Health, Melbourne, VIC, Australia, ⁵ Department of Psychiatry, University of Pittsburgh, Pittsburgh, PA, United States, ⁶ Division of Pharmacology, Faculty of Medicine, Tohoku Medical and Pharmaceutical University, Sendai, Japan

OPEN ACCESS

Edited by:

Naruhiko Sahara,
National Institutes for Quantum
and Radiological Science
and Technology, Japan

Reviewed by:

Sho Moriguchi,
Keio University Hospital, Japan
Etsuko Imabayashi,
Tokyo Metropolitan Institute
of Gerontology, Japan

*Correspondence:

Ryuichi Harada
ryuichi.harada.c8@tohoku.ac.jp
Nobuyuki Okamura
nookamura@tohoku-mpu.ac.jp

Specialty section:

This article was submitted to
Neurodegeneration,
a section of the journal
Frontiers in Neuroscience

Received: 02 November 2021

Accepted: 14 January 2022

Published: 08 February 2022

Citation:

Harada R, Furumoto S, Kudo Y,
Yanai K, Villemagne VL and
Okamura N (2022) Imaging
of Reactive Astroglialosis by Positron
Emission Tomography.
Front. Neurosci. 16:807435.
doi: 10.3389/fnins.2022.807435

Many neurodegenerative diseases are neuropathologically characterized by neuronal loss, gliosis, and the deposition of misfolded proteins such as β -amyloid (A β) plaques and tau tangles in Alzheimer's disease (AD). In postmortem AD brains, reactive astrocytes and activated microglia are observed surrounding A β plaques and tau tangles. These activated glial cells secrete pro-inflammatory cytokines and reactive oxygen species, which may contribute to neurodegeneration. Therefore, *in vivo* imaging of glial response by positron emission tomography (PET) combined with A β and tau PET would provide new insights to better understand the disease process, as well as aid in the differential diagnosis, and monitoring glial response disease-specific therapeutics. There are two promising targets proposed for imaging reactive astroglialosis: monoamine oxidase-B (MAO-B) and imidazoline₂ binding site (I₂BS), which are predominantly expressed in the mitochondrial membranes of astrocytes and are upregulated in various neurodegenerative conditions. PET tracers targeting these two MAO-B and I₂BS have been evaluated in humans. [¹⁸F]THK-5351, which was originally designed to target tau aggregates in AD, showed high affinity for MAO-B and clearly visualized reactive astrocytes in progressive supranuclear palsy (PSP). However, the lack of selectivity of [¹⁸F]THK-5351 binding to both MAO-B and tau, severely limits its clinical utility as a biomarker. Recently, [¹⁸F]SMBT-1 was developed as a selective and reversible MAO-B PET tracer via compound optimization of [¹⁸F]THK-5351. In this review, we summarize the strategy underlying molecular imaging of reactive astroglialosis and clinical studies using MAO-B and I₂BS PET tracers.

Keywords: reactive astroglialosis, MAO-B, imidazoline₂ binding site, PET, radiotracers

INTRODUCTION

Alzheimer's disease (AD) is neuropathologically characterized by neuronal loss, deposition of β -amyloid (A β) plaques, and neurofibrillary tangles (NFT) (Jellinger and Baner, 1998). Astroglialosis and microglialosis have been observed surrounding both dense-core A β plaques and NFT (Alibhai et al., 2018). Neuroinflammatory changes, characterized by reactive astrocytes and activated microglia, are considered to be a secondary process following A β and tau accumulation and contribute greatly to neurodegeneration throughout the course of AD (Ingelsson et al., 2004). Astrocytes are the most abundant glial cells in the brain, which are involved in a wide range of physiological functions including synaptic plasticity, the formation of astroglial-vascular

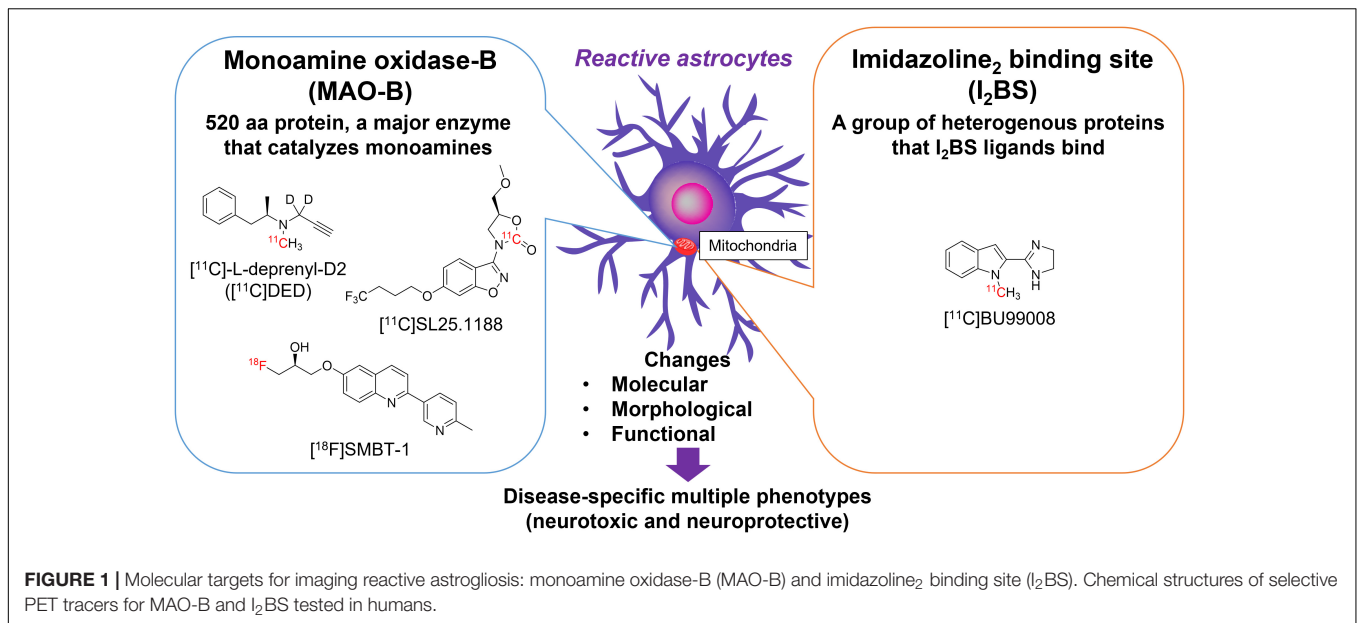
units, ion homeostasis, regulation of gliotransmitters such as glutamate and γ -aminobutyric acid (GABA), water transport, and regulation of local blood flow. When astrocytes respond to pathological conditions including traumatic brain injury, ischemia, infection, and misfolded protein accumulation, they exhibit morphological and phenotypic changes to transform into reactive astrocytes (Pekny et al., 2016). A recent consensus paper proposed that reactive astrogliosis should be defined as the spectrum of molecular, morphological, and functional changes in response to pathological conditions (Escartin et al., 2021). Reactive astrocytes display changes in gene expression and overexpress intermediate filaments such as glial fibrillary acid protein (GFAP), vimentin, and nestin. Reactive astrocytes secrete inflammatory mediators such as cytokines [interleukin-1 β (IL-1 β) and IL-6] and tumor necrosis factor- α (TNF- α), leading to the inflammatory, as observed in AD (Carter et al., 2019b). Reactive astrocytes have also been classified as neurotoxic (A1) and neuroprotective (A2) phenotypes. A1 astrocytes, observed in various neurodegenerative diseases, release the neurotoxic complement C3d and induce neuronal death. A2 astrocytes, commonly observed in ischemia, promote neuronal survival (Liddel et al., 2017). However, this binary classification does not truly reflect the wide spectrum of molecular, morphological, and functional changes observed in reactive astrogliosis. The term “astrogliosis” refers to a spectrum of potentially protective or deleterious pathways underlying complex phenotypic and functional changes reflecting both a loss of normal function and a gain of toxic function that can be region specific and associated with specific disease stages (Escartin et al., 2021). Therefore, a true classification is not possible given the variety of functions and morphologies, better served by the sum effect being preponderant protective or preponderant toxic (Escartin et al., 2021). Reactive astrogliosis is observed not only in AD, but also in various neurodegenerative diseases including amyotrophic lateral sclerosis (ALS), frontotemporal lobar degeneration (FTLD), Creutzfeldt-Jakob disease (CJD), progressive supranuclear palsy (PSP), Parkinson’s disease (PD), multiple system atrophy (MSA), and chronic traumatic encephalopathy (CTE), as well as in other neurological conditions such as epilepsy and stroke. Therefore, *in vivo* imaging of reactive astrocytes by positron emission tomography (PET) would provide new insights and a better understanding of the underlying disease process, aid in the differential diagnosis, and monitoring the glial response of disease-modifying therapeutics. In this review, we describe the recent advances in the development of PET tracers for imaging reactive astrocytes and the clinical applications of these new tracers.

MOLECULAR TARGETS IN THE DEVELOPMENT OF POSITRON EMISSION TOMOGRAPHY TRACER FOR IMAGING ASTROGLIOSIS

For imaging astrogliosis in the brain, translocator protein 18-kDa (TSPO) has been considered as a target in the development

of PET tracers (Escartin et al., 2021), although it is also widely recognized as an imaging marker for activated microglia. Since TSPO is overexpressed in both activated microglia and reactive astrocytes, there are technical limitations in achieving high glial cell-type specificity of PET tracers using TSPO as a molecular target. Furthermore, it is difficult to differentiate between neuroprotective and neurotoxic immune responses (Jain et al., 2020; Zhang et al., 2021). TSPO expression in AD and control brains was recently characterized in detail from postmortem brain samples (Gui et al., 2020). The findings of this study are as follows: (1) TSPO is expressed not only in microglia but also in astrocytes, endothelial cells, and vascular smooth muscle cells. (2) There is a substantial overlap in TSPO levels between control and AD brains. (3) The TSPO cortical burden did not correlate with the burden of activated microglia and reactive astrocytes. (4) The TSPO rs6971 Single Nucleotide Polymorphism (SNP) has been associated with a variable binding of TSPO radioligands, it does not affect neuropathological changes in AD. These findings suggest that a more specific and selective targets beyond TSPO are required for PET imaging of activated glial cells (Boche et al., 2019; Jain et al., 2020).

Reactive astrocytes are characterized by the overexpression of intermediate filaments such as GFAP, a gold standard marker of reactive astrocytes (Escartin et al., 2021). However, there are no available small molecular compounds for GFAP with high affinity and selectivity. Alternative surrogate targets of astrogliosis are monoamine oxidase-B (MAO-B) and imidazole binding sites (I₂BS), which are overexpressed in the outer mitochondrial membrane of reactive astrocytes (Ekblom et al., 1993; Regunathan et al., 1993; **Figure 1**). As many therapeutic drug candidates have been developed for pharmacological regulation of MAO-B and I₂BS, these compounds have been radiolabeled and tested as surrogate imaging probes for reactive astrogliosis (Carter et al., 2019b; **Figure 1**). MAO-B, a 520 amino acid protein, is the major enzyme that metabolizes monoamines such as dopamine, tyramine, and histamine in the human brain. MAO-B inhibitors such as selegiline (L-deprenyl), rasagiline, and safinamide have been used for the treatment of PD (Youdim et al., 2006). The crystal structures of human MAO-B revealed that irreversible MAO-B inhibitors such as L-deprenyl and rasagiline, which have an *N*-propargyl group covalently attached to the *N*5 atom of the flavin adenine dinucleotide (FAD) cofactor of MAO-B (Binda et al., 2002, 2004), while the reversible inhibitor safinamide binds non-covalently to MAO-B and occupy both the entrance and the substrate cavities (Binda et al., 2007). MAO-B is predominantly expressed in the outer membrane of the mitochondria in astrocytes but also in monoaminergic neurons, while it is much lower concentrations are found in oligodendrocytes, microglia, and endothelial cells (Levitt et al., 1982) (Brainrnaseq.org). Higher levels of MAO-B expression are observed in the basal forebrain, substantia nigra, basal ganglia, thalamus, and hippocampal uncus relative to the cerebellar cortex (Jossan et al., 1991a; Tong et al., 2013). There were significantly positive correlations with age (from 21 h to 99 years) for MAO-B in the frontal cortex ($r = 0.54$) (Tong et al., 2013). Age-related changes could be separated into three phases—within 1 year of age, 1–4 years, and thereafter. After



controlling for the effect of age, there was also a significant correlations in adults only (≥ 18 years, $r = 0.64$), childhood only (< 18 years, $r = 0.61$), or infancy only (< 1 year, $r = 0.82$). MAO-B levels are significantly correlated with GFAP immunoreactivity in the AD brain (Saura et al., 1994; Jo et al., 2014). Elevation of MAO-B levels in autopsy-confirmed AD brains has been consistently observed in mRNA levels and *in vitro* binding studies with MAO-B radioligands such as [^3H]-L-deprenyl and [^3H]lazabemide (Jossan et al., 1991b; Saura et al., 1994; Gulyas et al., 2011; Marutle et al., 2013; Jo et al., 2014; Ni et al., 2021). MAO-B was also upregulated in postmortem brain tissues from ALS, epilepsy, Parkinsonian syndromes such as PSP, PD, and MSA (Aquilonius et al., 1992; Kumlien et al., 1992; Ekblom et al., 1993; Tong et al., 2017).

I₂BS are an imidazoline binding sites compound of a group of heterogeneous proteins that are preferentially labeled by idazoxan and 2-(Benzofuran-2-yl)-2-imidazoline hydrochloride (2-BFI). The characteristics of imidazoline binding sites has been previously reviewed in detail (Bousquet et al., 2020). I₂BS are involved in regulation of GFAP expression and MAO-B activity (Olmos et al., 1994). Western blot analysis using polyclonal antiserum against idazoxan-binding proteins revealed four different protein bands (30, 45–57, 66, and 85 kDa) in rats and rabbits (Olmos et al., 1999). Brain creatine kinase was identified using a 2-BFI affinity column, which corresponded to an approximately 45 kDa band (Kimura et al., 2009). I₂BS are predominantly located at the outer mitochondrial membrane and are thought to be novel allosteric binding sites of MAO-A and MAO-B (Tesson et al., 1991, 1995; Parini et al., 1996). Both of MAO-B and I₂BS are not only expressed in astrocytes but also in neurons. 2-BFI binds to the tranylcypromine-inhibited-MAO-B form with high affinity, but presents low binding affinity to native human MAO-B. In addition, the crystal structure of the MAO-B-ligand complex demonstrated that 2-BFI binds to a site distinct from the substrate-binding cavity of MAO-B

(Bonivento et al., 2010). However, it is likely that proteins other than MAO also express I₂BS, as substantial specific radioligand binding remained in MAO knockout mice (Remaury et al., 2000; Anderson et al., 2006). The other bands detected by idazoxan remain unknown (Bousquet et al., 2020). [^3H]idazoxan binding in the human brain is greater in the basal ganglia, such as the caudate nucleus, putamen, substantia nigra, pons, and hippocampus than in the cerebellar cortex (De Vos et al., 1991). The density of I₂BS determined by [^3H]idazoxan was ~ 35 -fold lower than that of the MAO-B binding site determined by [^3H]Ro 19-6327 (a.k.a. lazabemide). As observed in MAO-B, the density of I₂BS increases linearly in an age-dependent manner in the frontal cortex during normal aging processes (Sastre and Garcia-Sevilla, 1993). The average increase per decade of I₂BS was 10.5 fmol/mg of protein ($\sim 16\%$ mean increase per decade between 20 and 70 years), while that of MAO-B was 44.7 fmol/mg of protein ($\sim 51\%$ mean increase per decade between 20 and 70 years). Therefore, age-related changes in brain I₂BS levels were 4-times lower than with those in MAO-B. Although the regional binding of radiotracers for MAO-B and I₂BS in the human brain is correlated with each other, the binding sites between MAO-B and I₂BS radiotracers are distinct (Sastre and Garcia-Sevilla, 1993). The density of [^3H]idazoxan binding in the AD brain is higher than that in the control brain (Ruiz et al., 1993). This finding is consistent with the results of western blot analysis using anti-imidazoline receptor protein anti-serum (Garcia-Sevilla et al., 1998). A novel PET tracer [^{11}C]BU99008, was developed as an I₂BS ligand. BU99008 possesses high affinity ($K_i = 1.4$ nM, $K_D = 1.3$ nM) and selectivity to I₂BS, compared with α_2 -adrenoceptor in rat brain ($K_i = 1,273$ nM) (Tyacke et al., 2012). Recently, BU99008 was established as an astroglial marker by analyzing postmortem AD brains (Kumar et al., 2021). The spatial distribution of [^3H]BU99008 was similar to that of the MAO-B radioligand [^3H]-L-deprenyl in large frozen sections from the control and AD groups. However, there was no

binding competition, suggesting that these two radioligands have different binding sites.

CLINICAL STUDIES USING POSITRON EMISSION TOMOGRAPHY RADIOTRACERS FOR MONOAMINE OXIDASE-B AND IMIDAZOLINE₂ BINDING SITE

Monoamine Oxidase-B: [¹¹C]-L-Deprenyl and [¹¹C]DED

Several PET tracers with high binding affinity to MAO-B or I₂BS have been investigated for the *in vivo* visualization of reactive astroglia. The first clinical study of MAO-B PET imaging was conducted using [¹¹C]-L-deprenyl, a selective and irreversible inhibitor of MAO-B (Fowler et al., 1987). However, [¹¹C]-L-deprenyl showed a rapid rate of first pass extraction relative to transport, resulting in a reduction in the sensitivity of the tracer in regions of high MAO-B concentrations, including the basal ganglia and thalamus on top of being influenced by blood flow. To minimize these effects, [¹¹C]-L-deprenyl D2 ([¹¹C]DED) was developed to improve tracer sensitivity (Fowler et al., 1995). [¹¹C]DED successfully reduced the first pass extraction of the tracer and improved sensitivity. There was a good correlation between MAO-B concentration ratios (ROI-to-cerebellum) and slope (*K_i*) ratios, which was estimated from graphical analysis for irreversible tracers. To date, [¹¹C]DED is the most widely used tracer for MAO-B PET in clinical studies to access MAO-B *in vivo* (Engler et al., 2012; Fowler et al., 2015; Rodriguez-Vieitez et al., 2016). MAO-B levels measured by [¹¹C]DED increased linearly in an age-dependent manner in whole brain regions during the normal aging process except for the cingulate gyrus (Fowler et al., 1997), consistent with postmortem data (Tong et al., 2013). Elevated [¹¹C]DED binding has been observed in several neurodegenerative conditions including traumatic brain injury (TBI), AD, ALS, and CJD (Fowler et al., 1999; Johansson et al., 2007; Santillo et al., 2011; Engler et al., 2012). However, another group reported that [¹¹C]DED binding was not elevated in patients with dementia, but was increased in PiB positive mild cognitive impairment (MCI) subjects (prodromal AD) (Carter et al., 2012). No regional correlations were found between [¹¹C]PiB, [¹¹C]DED, and [¹⁸F]FDG. On the other hands, some TBI patients showed an elevation of [¹¹C]DED in the regions corresponding to glucose hypometabolism (Fowler et al., 1999). [¹¹C]DED binding in the parahippocampus was negatively correlated with gray matter density in prodromal AD (Choo et al., 2014). They also reported that [¹¹C]DED binding was positively correlated with [¹¹C]PiB retention in the parahippocampus of AD. This region was also reported to significantly increase [¹¹C]PiB retention in AD dementia than prodromal AD (Nordberg et al., 2013). Furthermore, significant [¹¹C]DED binding was observed in pre-symptomatic mutation carriers of autosomal dominant AD (ADAD) that showed cerebral glucose metabolism were largely preserved (Scholl et al., 2015). Longitudinal studies in ADAD demonstrated

the positive rates of change in [¹¹C]PiB retention and negative rates of changes in [¹¹C]DED binding and [¹⁸F]FDG uptake in mutation carriers (Rodriguez-Vieitez et al., 2016). In addition, it showed high variability of [¹¹C]DED binding in mutation carriers and non-carriers (Rodriguez-Vieitez et al., 2016). Longitudinal reduction in [¹¹C]DED binding was also correlated with progressive cerebral glucose hypometabolism in pre-symptomatic mutation carriers (Carter et al., 2019a). Although it is considered that reduction of [¹¹C]DED binding is probably due to astrocytic dysfunction and atrophy by a downstream effect of the early MAO-B upregulation and a reflection of chronic neuroinflammation (Carter et al., 2019a), it remains unclear because many postmortem studies demonstrated the elevation of MAO-B levels in AD (Jossan et al., 1991b; Saura et al., 1994; Gulyas et al., 2011; Marutle et al., 2013; Ni et al., 2021). Furthermore, [¹¹C]DED presents difficulties in tracer binding quantification due to its irreversible binding kinetics and the presence of blood-brain barrier (BBB) penetrating radiolabeled metabolites including methamphetamine and amphetamine (Fowler et al., 1988; Azzaro et al., 2007; Narayanaswami et al., 2019), which bind to the monoamine transporter in the brain.

Monoamine Oxidase-B: [¹¹C]SL25.1188

As an alternative radiotracer, [¹¹C]SL25.1188 was developed as a MAO-B PET tracer and has shown more favorable reversible pharmacokinetics without BBB permeable radiolabeled metabolites in humans (Saba et al., 2010; Rusjan et al., 2014). A clinical study demonstrated that regional total distribution volume was highly correlated with previous reported MAO-B concentration using post-mortem brain samples, but the lack of *in vivo* blocking study with selective MAO-B inhibitors in humans. Assessment of MAO-B density was investigated in patients with major depressive disorder because serotonergic neurons also contain MAO-B. [¹¹C]SL25.1188 PET demonstrated greater MAO-B density in the prefrontal cortex of patients with major depressive disorder (Moriguchi et al., 2019). Very recently, a [¹¹C]SL25.1188 PET study has been reported that trending lower tracer uptake in posttraumatic stress disorder (PTSD), which is a debilitating mental health condition that results from exposure to traumatic events (Gill et al., 2021). Although [¹¹C]SL25.1188 looks a promising MAO-B PET tracer, it was mainly used in the studies focusing on psychiatric disorders and there are few reported clinical studies in neurodegenerative diseases.

Tau and Monoamine Oxidase-B: [¹⁸F]THK-5351

Although a 2-arylquinoline derivative [¹⁸F]THK-5351 was originally developed as a tau PET ligand (Harada et al., 2016; Tago et al., 2016), validation studies revealed off-target binding of [¹⁸F]THK-5351 to MAO-B (Ng et al., 2017; Harada et al., 2018). [¹⁸F]THK-5351 binds to MAO-B with high affinity and the *in vivo* [¹⁸F]THK-5351 binding was correlated with MAO-B levels in autopsy-confirmed AD and PSP patients (Harada et al., 2018; Ishiki et al., 2018). In addition, *in vivo* blocking studies with oral selegiline and rasagiline revealed specific binding of

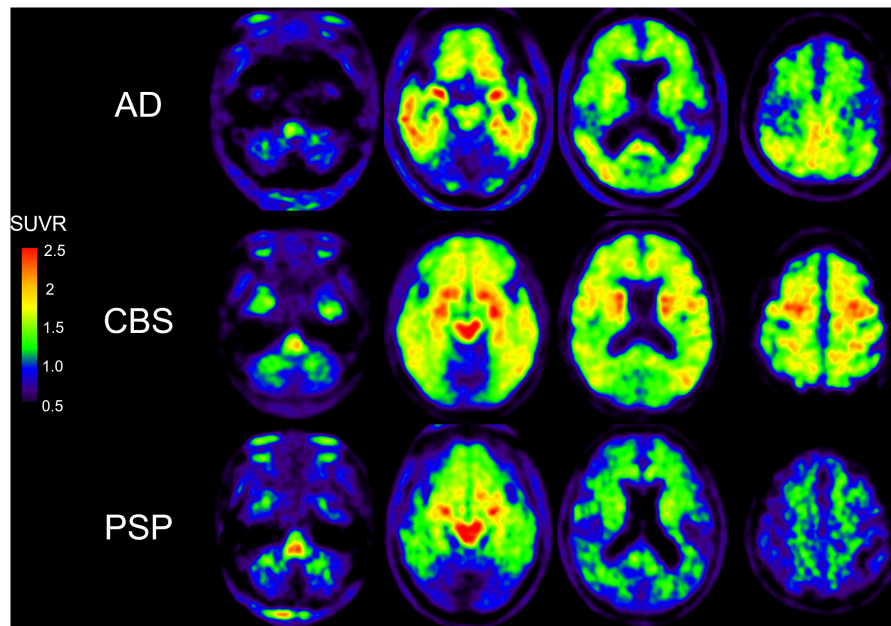


FIGURE 2 | [^{18}F]THK-5351 PET images in AD, CBS, and PSP subjects. [^{18}F]THK-5351 retention in the precentral gyrus clearly can distinguish CBS from PSP and AD. [^{18}F]THK-5351 retention in the midbrain distinguished PSP and CBS from AD (Okamura et al., 2018).

[^{18}F]THK-5351 to MAO-B in AD and PSP brains (Ng et al., 2017, 2019), where [^{18}F]THK-5351 binding was reduced on average by 37–52% in the post-selegiline scans and 53–89% in the post-rasagiline scans (Ng et al., 2017, 2019). These results suggested [^{18}F]THK-5351 would be useful for the evaluation of reactive astrogliosis and several researchers examined the potential clinical utility of [^{18}F]THK-5351 in various disease conditions including AD and non-AD conditions. Although there were a lot of limitations to interpret [^{18}F]THK-5351 PET images on the biological point of view due to the lack of selectivity, many clinical studies using [^{18}F]THK-5351 imply the association of reactive astrogliosis in various conditions. Clinical PET studies demonstrated high and different distribution of [^{18}F]THK-5351 retention in sites susceptible to tau deposition in AD and non-AD conditions such as Parkinsonian syndromes (Harada et al., 2016; Kikuchi et al., 2016; Brendel et al., 2017; Ishiki et al., 2017; Shimizu et al., 2018; Schonecker et al., 2019; Hsu et al., 2020; Ezura et al., 2021; **Figure 2**). Furthermore, [^{18}F]THK-5351 retention mirrors glucose hypometabolism measured with [^{18}F]fluorodeoxyglucose in the focal variants of AD (Kang et al., 2017; Park et al., 2021). [^{18}F]THK-5351 PET studies in AD also showed different tracer retention in three distinct subtypes of AD: medial temporal dominant subtype, parietal-dominant subtype, and diffuse atrophy subtype (Jeon et al., 2019). Semantic variant primary progressive aphasia (svPPA) is typically associated with frontotemporal lobar degeneration with the accumulation of TDP-43 (FTLD-TDP type C), and is not commonly due to primary tauopathy or AD (Grossman, 2010). In svPPA patients, [^{18}F]THK-5351 demonstrated that elevated retention in the anteroinferior and lateral temporal cortices compared with normal control, and in the left inferior and

temporal polar region compared with AD (Kobayashi et al., 2018; Lee et al., 2018; Schaeffer et al., 2018; Takaya et al., 2018; Son et al., 2019). [^{18}F]THK-5351 showed remarkable retention in ALS and multiple sclerosis (Ishibashi et al., 2020; Higashihara et al., 2021; Saitoh et al., 2021). As observed in [^{11}C]DED PET study (Engler et al., 2012), [^{18}F]THK-5351 retention was elevated in autopsy-confirmed sporadic CJD patient (Kim et al., 2019). Neuropathological examination of this case showed abundant MAO-B expressing reactive astrogliosis and no remarkable tau deposition. These reports indicate that [^{18}F]THK-5351 PET can detect overexpressed MAO-B in reactive astrocytes *in vivo*. [^{18}F]THK-5351 PET has also been applied for clinical assessment in non-neurodegenerative diseases. In a patient who suffered a middle cerebral artery infarction, PET image showed intense [^{18}F]THK-5351 retention along the ipsilateral pyramidal tract, likely reflecting the gliosis accompanying Wallerian degeneration (Ishibashi et al., 2017). [^{18}F]THK-5351 retention in ischemic stroke patients was elevated in peristroke areas, but most importantly, in areas remote from the stroke lesion, suggesting that [^{18}F]THK-5351 PET reflects gliosis associated with widespread ischemia-related and associated with microstructural disruption (Huang et al., 2020). Prominent [^{18}F]THK-5351 retention was also reported in a patient after traumatic brain injuries (Uchida et al., 2021) and in a patient with glioblastoma and associated gliosis (Tago et al., 2019; Mitamura et al., 2021).

Imidazoline₂ Binding Site: [^{11}C]BU99008

Compared to MAO-B PET tracer, only [^{11}C]BU99008 was tested in humans as a PET tracer for imaging I₂BS. BU99008 was labeled with carbon-11 and investigated using PET (Kealey et al., 2013).

[¹¹C]BU99008 showed a robust brain entry after intravenous administration and high retention in the basal ganglia, moderate in the cortex, and lowest in the cerebellum in porcine, rhesus monkey, and humans (Parker et al., 2014; Tyacke et al., 2018). These findings were consistent with the reported *in vitro* distribution of I₂BS in the brain. The *in vivo* binding of [¹¹C]BU99008 was blocked by pretreatment with idazoxan, but not with the non-selective MAO inhibitor, isocarboxazid, suggesting high selectivity of this tracer to I₂BS in humans (Tyacke et al., 2018). After testing human biodistribution and radiation dosimetry of [¹¹C]BU99008 (Venkataraman et al., 2018), clinical studies were expanded to the patients with neurodegenerative diseases. Early PD patients showed an elevation of [¹¹C]BU99008 in frontal, temporal, parietal, and occipital cortical regions, while moderate/advanced PD patients showed a reduction of [¹¹C]BU99008 uptake across the whole brain (Wilson et al., 2019). A recent [¹¹C]BU99008 PET study in AD demonstrated higher tracer uptake in frontal, temporal, occipital, and medial temporal regions of Aβ-positive cognitively impaired subjects. There was a positive correlation between [¹¹C]BU99008 and [¹⁸F]Florbetaben binding in cognitively impaired subjects (Calsolaro et al., 2021). Since there are a few reports about [¹¹C]BU99008 clinical PET studies, further studies are required.

Comparison of Monoamine Oxidase-B and Imidazoline₂ Binding Site Positron Emission Tomography Tracers

Comparison of PET tracers for imaging MAO-B and I₂BS tested in humans were shown in **Table 1**. Although there are several clinically available MAO-B PET tracers and single I₂BS PET tracer, the performance of each tracers remains unknown in various conditions. A direct head-to-head comparison study between [¹¹C]-L-deprenyl (prototype of [¹¹C]DED) and [¹⁸F]THK-5351 in patients with non-AD neurological disorders whose brains are not expected to harbor tau pathology concluded that [¹⁸F]THK-5351 was superior to [¹¹C]-L-deprenyl for visualizing lesions undergoing reactive astroglia (Ishibashi et al., 2021). [¹⁸F]THK-5351 PET (*B_P_{ND}* and SUV) images clearly identified the affected regions undergoing astroglia in patients with cerebral

infarction, progressive multifocal leukoencephalopathy, and multiple sclerosis. Although [¹¹C]-L-deprenyl *K_i/k₁* maps were similar to [¹⁸F]THK-5351 PET images, the signal-to-noise ratio of [¹¹C]-L-deprenyl PET images was much lower than that of [¹⁸F]THK-5351 PET images. *K_i* maps and SUV images of [¹¹C]-L-deprenyl seemed to be affected by blood flow due to its irreversible binding properties as described above. [¹¹C]-L-deprenyl shows irreversible binding kinetics, while [¹¹C]SL25.1188 shows reversible binding kinetics as like [¹⁸F]THK-5351. Future head-to-head comparison studies are required to characterize the performance of reversible MAO-B PET tracers. In addition, head-to-head studies between I₂BS and MAO-B PET tracers to compare degree of tracer binding as well as regional distribution of the tracers are also certainly warranted. Considering the non-selective binding properties of [¹⁸F]THK-5351 to MAO-B and AD-tau, [¹⁸F]THK-5351 is likely to be useful in non-AD patients whose brains are not expected to harbor tau pathology. However, it is important to ensure the specificity and sensitivity of MAO-B PET tracers because astrocyte dysfunction occurs at the early disease stages across the AD spectrum (Leclerc and Abulrob, 2013).

Recent Progress in the Development of Novel Monoamine Oxidase-B Tracers

Although several PET tracers have been evaluated for imaging reactive astroglia in humans, most of them were labeled with carbon-11, which limits widespread clinical applications. ¹⁸F-labeled MAO-B PET tracers such as [¹⁸F]fluorodeprenyl, [¹⁸F]fluororasagiline, [¹⁸F]fluorodeprenyl-D2, and [¹⁸F]fluororasagiline-D2 have been developed based on MAO-B inhibitors (Nag et al., 2011, 2012a,b, 2013, 2016). However, these tracers possess irreversible binding properties against MAO-B. More recently, development of reversible ¹⁸F-labeled MAO-B tracers such as [¹⁸F]FSL25.1188, [¹⁸F]FBPO, and [¹⁸F]GHC200449 have been reported (Dahl et al., 2019; Yoshimoto et al., 2019; Nag et al., 2020; Dukic-Stefanovic et al., 2021).

MAO-B contains β-sheet rich regions that create a substrate cavity space and an entrance cavity space (**Figure 3**). Irreversible MAO-B inhibitors contain an *N*-propargyl group covalently

TABLE 1 | Comparison among MAO-B and I₂BS PET tracers under various conditions in clinical studies.

Tracers	Targets	Binding kinetics	Tracer uptake (Compared with age-matched control)
[¹¹ C]DED	MAO-B	Irreversible	No significant difference in AD Increase in Aβ + MCI, pre-symptomatic mutation carrier of ADAD, ALS, CJD, TBI
[¹¹ C]SL25.1188	MAO-B	Reversible	Increase in major depressive disorder A trend of decrease in PTSD
[¹¹ C]BU99008	I ₂ BS	Reversible	Increase in early PD and Aβ + prodromal AD Decrease in late PD
[¹⁸ F]THK-5351	Tau/MAO-B	Reversible	Increase in AD*, CBS*, PSP, MSA-C, SD, bvFTD, ALS, CJD, TBI, cerebral infarction, progressive multifocal leukoencephalopathy, multiple sclerosis, ischemic stroke, glioma associated with gliosis
[¹⁸ F]SMBT-1	MAO-B	Reversible	Increase in AD

*The uptake may be due to binding to tau aggregates.

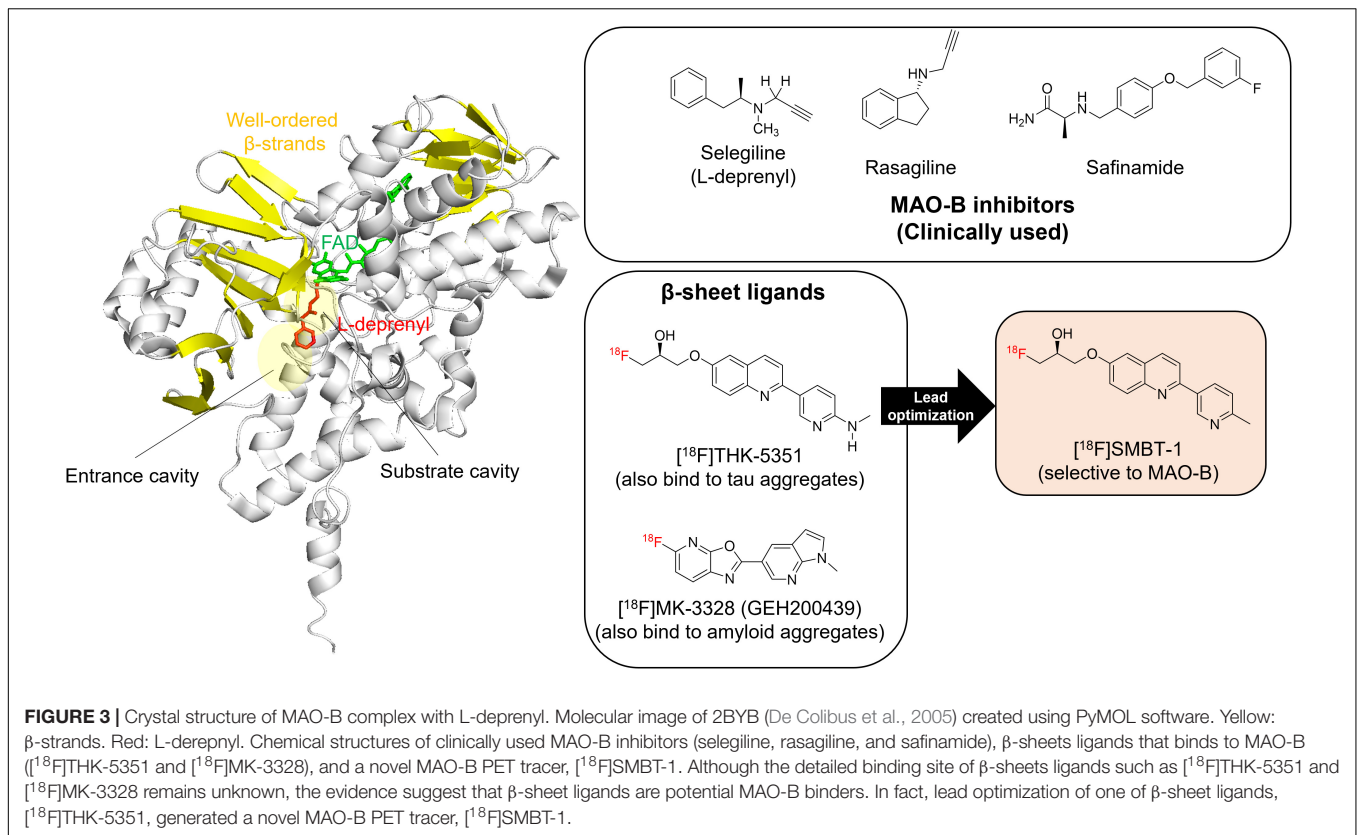
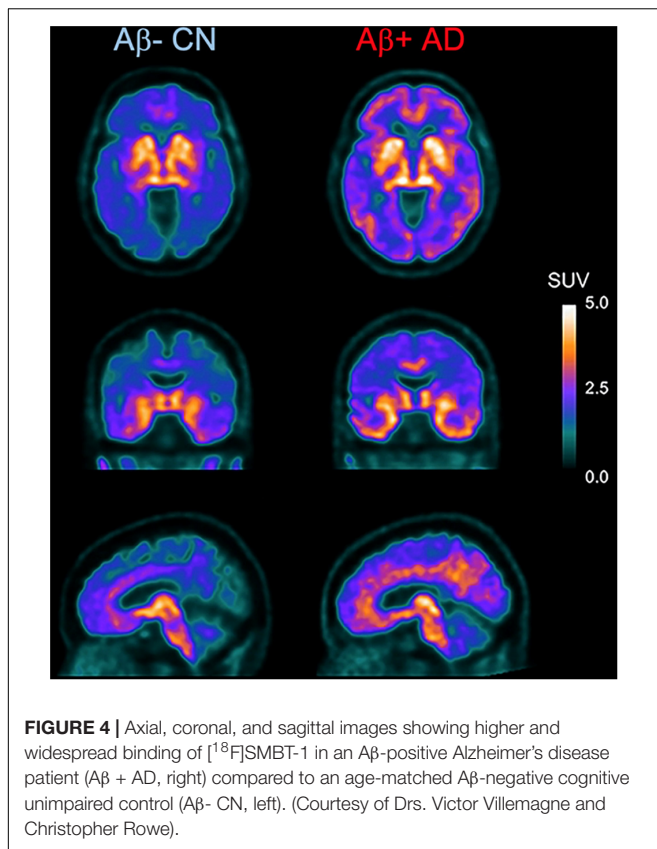


FIGURE 3 | Crystal structure of MAO-B complex with L-deprenyl. Molecular image of 2BYB (De Colibus et al., 2005) created using PyMOL software. Yellow: β -strands. Red: L-deprenyl. Chemical structures of clinically used MAO-B inhibitors (selegiline, rasagiline, and safinamide), β -sheet ligands that binds to MAO-B ($[^{18}\text{F}]\text{THK-5351}$ and $[^{18}\text{F}]\text{MK-3328}$), and a novel MAO-B PET tracer, $[^{18}\text{F}]\text{SMBT-1}$. Although the detailed binding site of β -sheet ligands such as $[^{18}\text{F}]\text{THK-5351}$ and $[^{18}\text{F}]\text{MK-3328}$ remains unknown, the evidence suggest that β -sheet ligands are potential MAO-B binders. In fact, lead optimization of one of β -sheet ligands, $[^{18}\text{F}]\text{THK-5351}$, generated a novel MAO-B PET tracer, $[^{18}\text{F}]\text{SMBT-1}$.

attached to the N5 atom of the FAD cofactor of MAO-B, which is adjacent to β -sheet rich region. *In vitro* competitive binding assays indicated that THK-5351 exhibits competitive binding with both reversible and irreversible MAO-B inhibitors. A docking simulation was reported to understand the binding site of tau PET tracers including THK-5351 in MAO-B (Murugan et al., 2019). Although the detailed binding site of THK-5351 remains unknown, the evidence suggest that β -sheet ligands are potential MAO binders (Figure 3). In fact, validation studies of A β and tau PET tracers identified that some of them possess high binding affinity against MAO-B (Sur et al., 2010; Ng et al., 2017; Harada et al., 2018; Vermeiren et al., 2018; Drake et al., 2019). $[^{18}\text{F}]\text{MK-3328}$ (GEH200439), which was originally developed as a candidate for A β PET tracer, showed the interaction with MAO-B in human brains (Sur et al., 2010; Figure 3). However, this tracer showed high non-specific binding in the white matter (Hostetler et al., 2011; Nag et al., 2020).

As mentioned above, $[^{18}\text{F}]\text{THK-5351}$ PET can detect MAO-B with highly sensitivity. Therefore, we developed a novel reversible and selective MAO-B tracer, $[^{18}\text{F}]\text{SMBT-1}$ through compound optimization of $[^{18}\text{F}]\text{THK-5351}$, which is one of the β -sheet ligands. $[^{18}\text{F}]\text{THK-5351}$ possess a good pharmacokinetic (PK) profile, reflected in high brain uptake and rapid washout without defluorination in humans (Lockhart et al., 2016; Betthausen et al., 2017; Hsiao et al., 2017). Our strategy was to develop compounds that reduce the binding affinity to tau aggregates while preserving the binding affinity to MAO-B and the good PK

profile. Previous structure–activity relationship (SAR) analysis of 2-arylquinoline derivatives showed that the 2-amino group on the pyridine ring of 2-arylquinoline derivatives was essential for binding to tau aggregates. SAR analysis of MAO-B using our compound library revealed that the hydroxy group in the 3-fluoro-2-hydroxypropyl (FHP) group of 2-arylquinoline plays an important role in achieving high binding affinity for MAO-B. Therefore, we synthesized 2-arylquinoline derivatives that has FHP group. Lead optimization process revealed that the 2-methylpyridine derivative ($[^{18}\text{F}]\text{SMBT-1}$) was the best candidate for imaging MAO-B *in vivo* (Harada et al., 2021). Preclinical studies of $[^{18}\text{F}]\text{SMBT-1}$ demonstrated that high binding affinity and high binding selectivity to MAO-B with low non-specific binding as well as good PK and metabolic profiles (Harada et al., 2021). Preliminary cross-sectional human PET studies in a wide range of ages are indicating that $[^{18}\text{F}]\text{SMBT-1}$ is a selective MAO-B tracer with low non-specific binding, high entry into the brain while displaying favorable reversible kinetics, and have significantly higher binding in A β + AD (Figure 4) and A β + cognitively unimpaired controls (Villemagne et al., 2022), similarly to what has been reported with plasma GFAP (Verberk et al., 2020; Chatterjee et al., 2021). These findings suggest that reactive astroglia as measured by MAO-B through $[^{18}\text{F}]\text{SMBT-1}$ is associated with early A β accumulation, providing strong support for its use as surrogate marker of astroglia. Ongoing clinical studies will also clarify the potential usefulness of $[^{18}\text{F}]\text{SMBT-1}$ in other disease conditions.



Imaging of Monoamine Oxidase-B in Animal Models: Implication of Reactive Astrogliosis

Although there are several clinical studies using [¹¹C]DED, only several preclinical studies have been reported. Aβ deposition and astrogliosis in APP_{Swe} mice were evaluated using the Aβ PET tracer [¹¹C]AZD2184 and [¹¹C]DED. Significant [¹¹C]DED binding was observed before significant accumulation of Aβ deposits in the brain, although the *in vivo* PET finding was inconsistent with the *in vitro* autoradiography results of [³H]-L-deprenyl (Rodriguez-Vieitez et al., 2015). Another preclinical imaging study using [¹¹C]DED in APP_{ArcSwe} mice showed a trend of increasing tracer binding in APP_{ArcSwe} mice compared with age-matched wildtype mice, but there was large intragroup variation (Olsen et al., 2018). There was little co-localization between MAO-B and GFAP in these mice, in contrast with good correlation between MAO-B and GFAP in postmortem human brain tissues (Levitt et al., 1982; Jo et al., 2014). This discrepancy could be due to species differences of MAO-B between mice and humans. MAO-B is predominantly expressed in humans and not in rodents. MAO-B expression levels in rodents were 2.5–4.7-fold lower than those in humans (Saura et al., 1992). A head-to-head comparison study of [¹¹C]-L-deprenyl, [¹¹C]DED, and [¹¹C]SL25.1188 in unilateral intrastratial lipopolysaccharide (LPS) injected rat model demonstrated that specific binding was only observed in [¹¹C]-L-deprenyl (Narayanaswami et al., 2021). They explained the reasons due to faster metabolism

of [¹¹C]DED in rats and higher non-specific binding and lower binding affinity of [¹¹C]SL25.1188 to rat brain tissues. [¹⁸F]FEPPA, one of the TSPO PET tracers, showed higher binding in the injection site at 1 week post-LPS injection, while [¹¹C]-L-deprenyl did not. However, although there were lower uptake of [¹⁸F]FEPPA at 1-month post-LPS injection than 1-week time point, [¹¹C]-L-deprenyl increased the binding in the 2-week and 1-month time points, suggesting increase of MAO-B expression is a later phase of neuroinflammation in this rat model. A study using *in vivo* two-photon microscopy demonstrated the close correlation between the MAO activity and AD progression (Kim et al., 2016). This study demonstrated that MAO activity started to increase in parallel with the deposition of Aβ plaques even in 4 month-old 5 × FAD mice, suggesting that MAO-B expression in reactive astrocytes occur at the early stages of disease in mice.

GFAP-positive reactive astrogliosis were observed not only in APP transgenic mice but also in other animal models such as doxycycline inducible astrocytic MAO-B transgenic mice (Mallajosyula et al., 2008), ischemia models (Boutin et al., 2015), LPS-injected animals (Ory et al., 2015), tau transgenic mice (Ramsden et al., 2005), and APP knock-in mice (Saito et al., 2014). Development of highly sensitive MAO-B tracers would allow for improved *in vivo* PET imaging in animal models. In addition, further studies are required to find other possible targets for imaging reactive astrogliosis and to develop a technique to discriminate between beneficial and toxic immune responses.

CONCLUSION

Reactive astrogliosis occurs commonly not only in AD but also in various neurological conditions. *In vivo* imaging of reactive astrogliosis is potentially useful for early and differential diagnosis, assessment of disease severity and evaluating drug efficacy. Several promising PET tracers for imaging reactive astrogliosis have emerged. Further clinical evaluation and preclinical validations are required to better understand the pathophysiological role(s) of reactive astrogliosis in neurodegeneration and to develop new treatment strategies.

AUTHOR CONTRIBUTIONS

RH and NO wrote the manuscript. SF, YK, KY, and VV revised the manuscript. All authors contributed to the article and approved the submitted version.

FUNDING

This study was supported by a Grant-in-Aid for Scientific Research (C) (20K08043), a Grant-in-Aid for Scientific Research (B) (18H02771), a Grant-in-Aid for Fostering Joint International Research (B) (19KK0212) from MEXT, and was supported by the Strategic Research Program for Brain Science (JP20dm0107157) from the Japan Agency for Medical Research and Development.

REFERENCES

- Alibhai, J. D., Diack, A. B., and Manson, J. C. (2018). Unravelling the glial response in the pathogenesis of Alzheimer's disease. *FASEB J.* 32, 5766–5777. doi: 10.1096/fj.201801360R
- Anderson, N. J., Seif, I., Nutt, D. J., Hudson, A. L., and Robinson, E. S. (2006). Autoradiographical distribution of imidazoline binding sites in monoamine oxidase A deficient mice. *J. Neurochem.* 96, 1551–1559. doi: 10.1111/j.1471-4159.2006.03662.x
- Aquilonius, S. M., Jossan, S. S., Ekblom, J. G., Askmark, H., and Gillberg, P. G. (1992). Increased binding of 3H-L-deprenyl in spinal cords from patients with amyotrophic lateral sclerosis as demonstrated by autoradiography. *J. Neural. Transm. Gen. Sect.* 89, 111–122. doi: 10.1007/BF01245357
- Azzaro, A. J., Ziemiak, J., Kemper, E., Campbell, B. J., and Vandenberg, C. (2007). Pharmacokinetics and absolute bioavailability of selegiline following treatment of healthy subjects with the selegiline transdermal system (6 mg/24 h): a comparison with oral selegiline capsules. *J. Clin. Pharmacol.* 47, 1256–1267. doi: 10.1177/0091270007304779
- Bethausser, T. J., Lao, P. J., Murali, D., Barnhart, T. E., Furumoto, S., Okamura, N., et al. (2017). In Vivo Comparison of Tau Radioligands (18)F-THK-5351 and (18)F-THK-5317. *J. Nucl. Med.* 58, 996–1002. doi: 10.2967/jnumed.116.182980
- Binda, C., Hubalek, F., Li, M., Herzig, Y., Sterling, J., Edmondson, D. E., et al. (2004). Crystal structures of monoamine oxidase B in complex with four inhibitors of the N-propargylaminoindan class. *J. Med. Chem.* 47, 1767–1774. doi: 10.1021/jm031087c
- Binda, C., Newton-Vinson, P., Hubalek, F., Edmondson, D. E., and Mattevi, A. (2002). Structure of human monoamine oxidase B, a drug target for the treatment of neurological disorders. *Nat. Struct. Biol.* 9, 22–26. doi: 10.1038/nsb732
- Binda, C., Wang, J., Pisani, L., Caccia, C., Carotti, A., Salvati, P., et al. (2007). Structures of human monoamine oxidase B complexes with selective noncovalent inhibitors: safinamide and coumarin analogs. *J. Med. Chem.* 50, 5848–5852. doi: 10.1021/jm070677y
- Boche, D., Gerhard, A., Rodriguez-Vieitez, E., and Faculty, M. (2019). Prospects and challenges of imaging neuroinflammation beyond TSPO in Alzheimer's disease. *Eur. J. Nucl. Med. Mol. Imaging* 46, 2831–2847. doi: 10.1007/s00259-019-04462-w
- Bonivento, D., Milczek, E. M., McDonald, G. R., Binda, C., Holt, A., Edmondson, D. E., et al. (2010). Potentiation of ligand binding through cooperative effects in monoamine oxidase B. *J. Biol. Chem.* 285, 36849–36856. doi: 10.1074/jbc.M110.169482
- Bousquet, P., Hudson, A., Garcia-Sevilla, J. A., and Li, J. X. (2020). Imidazoline receptor system: the past, the present, and the future. *Pharmacol. Rev.* 72, 50–79. doi: 10.1124/pr.118.016311
- Boutin, H., Murray, K., Pradillo, J., Maroy, R., Smigova, A., Gerhard, A., et al. (2015). 18F-GE-180: a novel TSPO radiotracer compared to 11C-R-PK11195 in a preclinical model of stroke. *Eur. J. Nucl. Med. Mol. Imaging* 42, 503–511. doi: 10.1007/s00259-014-2939-8
- Brendel, M., Schonecker, S., Hoglinger, G., Lindner, S., Havla, J., Blautzik, J., et al. (2017). [18F]-THK5351 PET correlates with topology and symptom severity in progressive supranuclear palsy. *Front. Aging Neurosci.* 9:440. doi: 10.3389/fnagi.2017.00440
- Calzolaro, V., Matthews, P. M., Donat, C. K., Livingston, N. R., Femminella, G. D., Guedes, S. S., et al. (2021). Astrocyte reactivity with late-onset cognitive impairment assessed in vivo using ¹¹C-BU99008 PET and its relationship with amyloid load. *Mol. Psychiatry* 26, 5848–5855. doi: 10.1038/s41380-021-01193-z
- Carter, S. F., Herholz, K., Rosa-Neto, P., Pellerin, L., Nordberg, A., and Zimmer, E. R. (2019b). Astrocyte biomarkers in Alzheimer's disease. *Trends Mol. Med.* 25, 77–95.
- Carter, S. F., Chiotis, K., Nordberg, A., and Rodriguez-Vieitez, E. (2019a). Longitudinal association between astrocyte function and glucose metabolism in autosomal dominant Alzheimer's disease. *Eur. J. Nucl. Med. Mol. Imaging* 46, 348–356. doi: 10.1007/s00259-018-4217-7
- Carter, S. F., Scholl, M., Almkvist, O., Wall, A., Engler, H., Langstrom, B., et al. (2012). Evidence for astrocytosis in prodromal Alzheimer disease provided by 11C-deuterium-L-deprenyl: a multitracers PET paradigm combining 11C-Pittsburgh compound B and 18F-FDG. *J. Nucl. Med.* 53, 37–46. doi: 10.2967/jnumed.110.087031
- Chatterjee, P., Pedrini, S., Stoops, E., Goozee, K., Villemagne, V. L., Asih, P. R., et al. (2021). Plasma glial fibrillary acidic protein is elevated in cognitively normal older adults at risk of Alzheimer's disease. *Transl. Psychiatry* 11:27. doi: 10.1038/s41398-020-01137-1
- Choo, I. L., Carter, S. F., Scholl, M. L., and Nordberg, A. (2014). Astrocytosis measured by ¹¹C-deprenyl PET correlates with decrease in gray matter density in the parahippocampus of prodromal Alzheimer's patients. *Eur. J. Nucl. Med. Mol. Imaging* 41, 2120–2126. doi: 10.1007/s00259-014-2859-7
- Dahl, K., Bernard-Gauthier, V., Nag, S., Varnas, K., Narayanaswami, V., Mahdi Moein, M., et al. (2019). Synthesis and preclinical evaluation of [18F]FSL25.1188, a reversible PET radioligand for monoamine oxidase-B. *Bioorg. Med. Chem. Lett.* 29, 1624–1627. doi: 10.1016/j.bmcl.2019.04.040
- De Colibus, L., Li, M., Binda, C., Lustig, A., Edmondson, D. E., and Mattevi, A. (2005). Three-dimensional structure of human monoamine oxidase A (MAO A): relation to the structures of rat MAO A and human MAO B. *Proc. Natl. Acad. Sci. U. S. A.* 102, 12684–12689. doi: 10.1073/pnas.0505975102
- De Vos, H., Convents, A., De Keyser, J., De Backer, J. P., Van Megen, I. J., Ebinger, G., et al. (1991). Autoradiographic distribution of alpha 2 adrenoceptors, NAIBS, and 5-HT1A receptors in human brain using [3H]idazoxan and [3H]rauwolscine. *Brain Res.* 566, 13–20. doi: 10.1016/0006-8993(91)91675-q
- Drake, L. R., Pham, J. M., Desmond, T. J., Mossine, A. V., Lee, S. J., Kilbourn, M. R., et al. (2019). Identification of AV-1451 as a weak, nonselective inhibitor of monoamine oxidase. *ACS Chem. Neurosci.* 10, 3839–3846. doi: 10.1021/acschemneuro.9b00326
- Dukic-Stefanovic, S., Hang Lai, T., Toussaint, M., Clauss, O., Jevtic, I. I., Penjisevic, J. Z., et al. (2021). In vitro and in vivo evaluation of fluorinated indanone derivatives as potential positron emission tomography agents for the imaging of monoamine oxidase B in the brain. *Bioorg. Med. Chem. Lett.* 48:128254. doi: 10.1016/j.bmcl.2021.128254
- Ekblom, J., Jossan, S. S., Bergstrom, M., Orelund, L., Walum, E., and Aquilonius, S. M. (1993). Monoamine oxidase-B in astrocytes. *Glia* 8, 122–132. doi: 10.1002/glia.440080208
- Engler, H., Nennesmo, I., Kumlien, E., Gambini, J. P., Lundberg, P., Savitcheva, I., et al. (2012). Imaging astrocytosis with PET in Creutzfeldt-Jakob disease: case report with histopathological findings. *Int. J. Clin. Exp. Med.* 5, 201–207.
- Escartin, C., Galea, E., Lakatos, A., O'callaghan, J. P., Petzold, G. C., Serrano-Pozo, A., et al. (2021). Reactive astrocyte nomenclature, definitions, and future directions. *Nat. Neurosci.* 24, 312–325. doi: 10.1038/s41593-020-00783-4
- Ezura, M., Kikuchi, A., Okamura, N., Ishiki, A., Hasegawa, T., Harada, R., et al. (2021). ¹⁸F-THK5351 positron emission tomography imaging in neurodegenerative tauopathies. *Front. Aging Neurosci.* 13:761010. doi: 10.3389/fnagi.2021.761010
- Fowler, J. S., Logan, J., Shumay, E., Alia-Klein, N., Wang, G. J., and Volkow, N. D. (2015). Monoamine oxidase: radiotracer chemistry and human studies. *J. Labelled Comp. Radiopharm.* 58, 51–64. doi: 10.1002/jlcr.3247
- Fowler, J. S., Macgregor, R. R., Wolf, A. P., Arnett, C. D., Dewey, S. L., Schlyer, D., et al. (1987). Mapping human brain monoamine oxidase A and B with 11C-labeled suicide inactivators and PET. *Science* 235, 481–485. doi: 10.1126/science.3099392
- Fowler, J. S., Volkow, N. D., Cilelto, R., Wang, G. J., Felder, C., and Logan, J. (1999). Comparison of brain glucose metabolism and monoamine oxidase B (MAO B) in traumatic brain injury. *Clin. Positron Imaging* 2, 71–79. doi: 10.1016/s1095-0397(99)00010-2
- Fowler, J. S., Volkow, N. D., Wang, G. J., Logan, J., Pappas, N., Shea, C., et al. (1997). Age-related increases in brain monoamine oxidase B in living healthy human subjects. *Neurobiol. Aging* 18, 431–435. doi: 10.1016/s0197-4580(97)00037-7
- Fowler, J. S., Wang, G. J., Logan, J., Xie, S., Volkow, N. D., Macgregor, R. R., et al. (1995). Selective reduction of radiotracer trapping by deuterium substitution:

- comparison of carbon-11-L-deprenyl and carbon-11-deprenyl-D2 for MAO B mapping. *J. Nucl. Med.* 36, 1255–1262.
- Fowler, J. S., Wolf, A. P., Macgregor, R. R., Dewey, S. L., Logan, J., Schlyer, D. J., et al. (1988). Mechanistic positron emission tomography studies: demonstration of a deuterium isotope effect in the monoamine oxidase-catalyzed binding of [¹¹C]-deprenyl in living baboon brain. *J. Neurochem.* 51, 1524–1534. doi: 10.1111/j.1471-4159.1988.tb01121.x
- García-Sevilla, J. A., Escriba, P. V., Walzer, C., Bouras, C., and Guimon, J. (1998). Imidazoline receptor proteins in brains of patients with Alzheimer's disease. *Neurosci. Lett.* 247, 95–98. doi: 10.1016/s0304-3940(98)00265-1
- Gill, T., Watling, S. E., Richardson, J. D., McCluskey, T., Tong, J., Meyer, J. H., et al. (2021). Imaging of astrocytes in posttraumatic stress disorder: a PET study with the monoamine oxidase B radioligand [¹¹C]SL25.1188. *Eur. Neuropsychopharmacol.* 54, 54–61. doi: 10.1016/j.euroneuro.2021.10.006
- Grossman, M. (2010). Primary progressive aphasia: clinicopathological correlations. *Nat. Rev. Neurol.* 6, 88–97. doi: 10.1038/nrneuro.2009.216
- Gui, Y., Marks, J. D., Das, S., Hyman, B. T., and Serrano-Pozo, A. (2020). Characterization of the 18 kDa translocator protein (TSPO) expression in post-mortem normal and Alzheimer's disease brains. *Brain Pathol.* 30, 151–164. doi: 10.1111/bpa.12763
- Gulyas, B., Pavlova, E., Kasa, P., Gulya, K., Bakota, L., Varszegi, S., et al. (2011). Activated MAO-B in the brain of Alzheimer patients, demonstrated by [¹¹C]-L-deprenyl using whole hemisphere autoradiography. *Neurochem. Int.* 58, 60–68. doi: 10.1016/j.neuint.2010.10.013
- Harada, R., Hayakawa, Y., Ezura, M., Lerdsiriruk, P., Du, Y., Ishikawa, Y., et al. (2021). ¹⁸F-SMBT-1: a selective and reversible PET tracer for monoamine oxidase-B imaging. *J. Nucl. Med.* 62, 253–258.
- Harada, R., Ishiki, A., Kai, H., Sato, N., Furukawa, K., Furumoto, S., et al. (2018). Correlations of ¹⁸F-THK5351 PET with postmortem burden of tau and astroglia in Alzheimer disease. *J. Nucl. Med.* 59, 671–674. doi: 10.2967/jnumed.117.197426
- Harada, R., Okamura, N., Furumoto, S., Furukawa, K., Ishiki, A., Tomita, N., et al. (2016). ¹⁸F-THK5351: a novel PET radiotracer for imaging neurofibrillary pathology in Alzheimer disease. *J. Nucl. Med.* 57, 208–214. doi: 10.2967/jnumed.115.164848
- Higashihara, M., Ishibashi, K., Tokumaru, A. M., Iwata, A., and Ishii, K. (2021). ¹⁸F-THK5351 PET can identify core lesions in different amyotrophic lateral sclerosis phenotypes. *Clin. Nucl. Med.* 46, e582–e583. doi: 10.1097/RLU.0000000000003755
- Hostetler, E. D., Sanabria-Bohorquez, S., Fan, H., Zeng, Z., Gammage, L., Miller, P., et al. (2011). [¹⁸F]Fluoroazabenzoxazoles as potential amyloid plaque PET tracers: synthesis and in vivo evaluation in rhesus monkey. *Nucl. Med. Biol.* 38, 1193–1203. doi: 10.1016/j.nucmedbio.2011.04.004
- Hsiao, I. T., Lin, K. J., Huang, K. L., Huang, C. C., Chen, H. S., Wey, S. P., et al. (2017). Biodistribution and radiation dosimetry for the tau tracer ¹⁸F-THK-5351 in healthy human subjects. *J. Nucl. Med.* 58, 1498–1503. doi: 10.2967/jnumed.116.189126
- Hsu, J. L., Chen, S. H., Hsiao, I. T., Lu, C. S., Yen, T. C., Okamura, N., et al. (2020). ¹⁸F-THK5351 PET imaging in patients with progressive supranuclear palsy: associations with core domains and diagnostic certainty. *Sci. Rep.* 10:19410.
- Huang, K. L., Hsiao, I. T., Ho, M. Y., Hsu, J. L., Chang, Y. J., Chang, T. Y., et al. (2020). Investigation of reactive astroglia effect on post-stroke cognitive impairment. *J. Neuroinflamm.* 17:308. doi: 10.1186/s12974-020-01985-0
- Ingelsson, M., Fukumoto, H., Newell, K. L., Growdon, J. H., Hedley-Whyte, E. T., Froesch, M. P., et al. (2004). Early Abeta accumulation and progressive synaptic loss, gliosis, and tangle formation in AD brain. *Neurology* 62, 925–931. doi: 10.1212/01.wnl.0000115115.98960.37
- Ishibashi, K., Kameyama, M., Miura, Y., Toyohara, J., and Ishii, K. (2021). Head-to-head comparison of the two MAO-B Radioligands, ¹⁸F-THK5351 and ¹¹C-L-Deprenyl, to visualize astroglia in patients with neurological disorders. *Clin. Nucl. Med.* 46, e31–e33. doi: 10.1097/RLU.0000000000003197
- Ishibashi, K., Kameyama, M., Tago, T., Toyohara, J., and Ishii, K. (2017). Potential use of ¹⁸F-THK5351 PET to identify wallerian degeneration of the pyramidal tract caused by cerebral infarction. *Clin. Nucl. Med.* 42, e523–e524. doi: 10.1097/RLU.0000000000001868
- Ishibashi, K., Miura, Y., Hirata, K., Toyohara, J., and Ishii, K. (2020). ¹⁸F-THK5351 PET can identify astroglia in multiple sclerosis plaques. *Clin. Nucl. Med.* 45, e98–e100. doi: 10.1097/RLU.0000000000002751
- Ishiki, A., Harada, R., Kai, H., Sato, N., Totsune, T., Tomita, N., et al. (2018). Neuroimaging-pathological correlations of [¹⁸F]THK5351 PET in progressive supranuclear palsy. *Acta Neuropathol. Commun.* 6:53. doi: 10.1186/s40478-018-0556-7
- Ishiki, A., Harada, R., Okamura, N., Tomita, N., Rowe, C. C., Villemagne, V. L., et al. (2017). Tau imaging with [¹⁸F]THK-5351 in progressive supranuclear palsy. *Eur. J. Neurol.* 24, 130–136. doi: 10.1111/ene.13164
- Jain, P., Chaney, A. M., Carlson, M. L., Jackson, I. M., Rao, A., and James, M. L. (2020). Neuroinflammation PET imaging: current opinion and future directions. *J. Nucl. Med.* 61, 1107–1112. doi: 10.2967/jnumed.119.229443
- Jellinger, K. A., and Bancher, C. (1998). Neuropathology of Alzheimer's disease: a critical update. *J. Neural. Transm. Suppl.* 54, 77–95. doi: 10.1007/978-3-7091-7508-8_8
- Jeon, S., Kang, J. M., Seo, S., Jeong, H. J., Funck, T., Lee, S. Y., et al. (2019). Topographical Heterogeneity of Alzheimer's disease based on MR Imaging, Tau PET, and Amyloid PET. *Front. Aging Neurosci.* 11:211. doi: 10.3389/fnagi.2019.00211
- Jo, S., Yarishkin, O., Hwang, Y. J., Chun, Y. E., Park, M., Woo, D. H., et al. (2014). GABA from reactive astrocytes impairs memory in mouse models of Alzheimer's disease. *Nat. Med.* 20, 886–896. doi: 10.1038/nm.3639
- Johansson, A., Engler, H., Blomquist, G., Scott, B., Wall, A., Aquilonius, S. M., et al. (2007). Evidence for astrocytosis in ALS demonstrated by [¹¹C](L)-deprenyl-D2 PET. *J. Nucl. Med.* 48, 17–22. doi: 10.1016/j.jns.2007.01.057
- Jossan, S. S., Gillberg, P. G., D'argy, R., Aquilonius, S. M., Langstrom, B., Halldin, C., et al. (1991a). Quantitative localization of human brain monoamine oxidase B by large section autoradiography using L-[³H]deprenyl. *Brain Res.* 547, 69–76. doi: 10.1016/0006-8993(91)90575-g
- Jossan, S. S., Gillberg, P. G., Gottfries, C. G., Karlsson, I., and Oreland, L. (1991b). Monoamine oxidase B in brains from patients with Alzheimer's disease: a biochemical and autoradiographical study. *Neuroscience* 45, 1–12. doi: 10.1016/0306-4522(91)90098-9
- Kang, J. M., Lee, S. Y., Seo, S., Jeong, H. J., Woo, S. H., Lee, H., et al. (2017). Tau positron emission tomography using [¹⁸F]THK5351 and cerebral glucose hypometabolism in Alzheimer's disease. *Neurobiol. Aging* 59, 210–219. doi: 10.1016/j.neurobiolaging.2017.08.008
- Kealey, S., Turner, E. M., Husbands, S. M., Salinas, C. A., Jakobsen, S., Tyacke, R. J., et al. (2013). Imaging imidazoline-12 binding sites in porcine brain using ¹¹C-BU99008. *J. Nucl. Med.* 54, 139–144. doi: 10.2967/jnumed.112.108258
- Kikuchi, A., Okamura, N., Hasegawa, T., Harada, R., Watanuki, S., Funaki, Y., et al. (2016). In vivo visualization of tau deposits in corticobasal syndrome by ¹⁸F-THK5351 PET. *Neurology* 87, 2309–2316. doi: 10.1212/WNL.0000000000003755
- Kim, D., Baik, S. H., Kang, S., Cho, S. W., Bae, J., Cha, M. Y., et al. (2016). Close correlation of monoamine oxidase activity with progress of Alzheimer's disease in mice, observed by in vivo two-photon imaging. *ACS Cent. Sci.* 2, 967–975. doi: 10.1021/acscentsci.6b00309
- Kim, H. J., Cho, H., Park, S., Jang, H., Ryu, Y. H., Choi, J. Y., et al. (2019). THK5351 and flortaucipir PET with pathological correlation in a Creutzfeldt-Jakob disease patient: a case report. *BMC Neurol.* 19:211. doi: 10.1186/s12883-019-1434-z
- Kimura, A., Tyacke, R. J., Robinson, J. J., Husbands, S. M., Minchin, M. C., Nutt, D. J., et al. (2009). Identification of an imidazoline binding protein: creatine kinase and an imidazoline-2 binding site. *Brain Res.* 1279, 21–28. doi: 10.1016/j.brainres.2009.04.044
- Kobayashi, R., Hayashi, H., Kawakatsu, S., Ishiki, A., Okamura, N., Arai, H., et al. (2018). [¹⁸F]THK-5351 PET imaging in early-stage semantic variant primary progressive aphasia: a report of two cases and a literature review. *BMC Neurol.* 18:109. doi: 10.1186/s12883-018-1115-3
- Kumar, A., Koistinen, N. A., Malarte, M. L., Nennesmo, I., Ingelsson, M., Ghetti, B., et al. (2021). Astroglial tracer BU99008 detects multiple binding sites in Alzheimer's disease brain. *Mol. Psychiatry* 26, 5833–5847. doi: 10.1038/s41380-021-01101-5

- Kumlien, E., Hilton-Brown, P., Spannare, B., and Gillberg, P. G. (1992). In vitro quantitative autoradiography of [3H]-L-deprenyl and [3H]-PK 11195 binding sites in human epileptic hippocampus. *Epilepsia* 33, 610–617. doi: 10.1111/j.1528-1157.1992.tb02336.x
- Leclerc, B., and Abulrob, A. (2013). Perspectives in molecular imaging using staging biomarkers and immunotherapies in Alzheimer's disease. *ScientificWorldJournal* 2013:589308. doi: 10.1155/2013/589308
- Lee, H., Seo, S., Lee, S. Y., Jeong, H. J., Woo, S. H., Lee, K. M., et al. (2018). [18F]-THK5351 PET imaging in patients with semantic variant primary progressive aphasia. *Alzheimer Dis. Assoc. Disord.* 32, 62–69. doi: 10.1097/WAD.0000000000000216
- Levitt, P., Pintar, J. E., and Breakefield, X. O. (1982). Immunocytochemical demonstration of monoamine oxidase B in brain astrocytes and serotonergic neurons. *Proc. Natl. Acad. Sci. U. S. A.* 79, 6385–6389. doi: 10.1073/pnas.79.20.6385
- Liddelov, S. A., Guttenplan, K. A., Clarke, L. E., Bennett, F. C., Bohlen, C. J., Schirmer, L., et al. (2017). Neurotoxic reactive astrocytes are induced by activated microglia. *Nature* 541, 481–487. doi: 10.1038/nature21029
- Lockhart, S. N., Baker, S. L., Okamura, N., Furukawa, K., Ishiki, A., Furumoto, S., et al. (2016). Dynamic PET measures of tau accumulation in cognitively normal older adults and Alzheimer's disease patients measured using [18F] THK-5351. *PLoS One* 11:e0158460. doi: 10.1371/journal.pone.0158460
- Mallajosyula, J. K., Kaur, D., Chinta, S. J., Rajagopalan, S., Rane, A., Nicholls, D. G., et al. (2008). MAO-B elevation in mouse brain astrocytes results in Parkinson's pathology. *PLoS One* 3:e1616. doi: 10.1371/journal.pone.0001616
- Marutle, A., Gillberg, P. G., Bergfors, A., Yu, W., Ni, R., Nennesmo, I., et al. (2013). ³H-deprenyl and ³H-PIB autoradiography show different laminar distributions of astroglia and fibrillar beta-amyloid in Alzheimer brain. *J. Neuroinflamm.* 10:90. doi: 10.1186/1742-2094-10-90
- Mitamura, K., Norikane, T., Yamamoto, Y., Miyake, K., and Nishiyama, Y. (2021). Increased uptake of 18F-THK5351 in glioblastoma but not in primary central nervous system lymphoma. *Clin. Nucl. Med.* 46, 772–773. doi: 10.1097/RLU.00000000000003699
- Moriguchi, S., Wilson, A. A., Miler, L., Rusjan, P. M., Vasdev, N., Kish, S. J., et al. (2019). Monoamine oxidase B total distribution volume in the prefrontal cortex of major depressive disorder: an [11C]SL25.1188 positron emission tomography study. *JAMA Psychiatry* 76, 634–641. doi: 10.1001/jamapsychiatry.2019.0044
- Murugan, N. A., Chiotis, K., Rodriguez-Vieitez, E., Lemoine, L., Agren, H., and Nordberg, A. (2019). Cross-interaction of tau PET tracers with monoamine oxidase B: evidence from in silico modelling and in vivo imaging. *Eur. J. Nucl. Med. Mol. Imaging* 46, 1369–1382. doi: 10.1007/s00259-019-04305-8
- Nag, S., Fazio, P., Lehmann, L., Ketschau, G., Heinrich, T., Thiele, A., et al. (2016). In Vivo and In Vitro characterization of a novel MAO-B Inhibitor Radioligand, 18F-labeled deuterated fluorodeprenyl. *J. Nucl. Med.* 57, 315–320. doi: 10.2967/jnumed.115.161083
- Nag, S., Jia, Z., Svedberg, M., Jackson, A., Ahmad, R., Luthra, S., et al. (2020). Synthesis and autoradiography of novel F-18 labeled reversible radioligands for detection of monoamine oxidase B. *ACS Chem. Neurosci.* 11, 4398–4404. doi: 10.1021/acscchemneuro.0c00631
- Nag, S., Lehmann, L., Heinrich, T., Thiele, A., Ketschau, G., Nakao, R., et al. (2011). Synthesis of three novel fluorine-18 labeled analogues of L-deprenyl for positron emission tomography (PET) studies of monoamine oxidase B (MAO-B). *J. Med. Chem.* 54, 7023–7029. doi: 10.1021/jm200710b
- Nag, S., Lehmann, L., Ketschau, G., Heinrich, T., Thiele, A., Varrone, A., et al. (2012a). Synthesis and evaluation of [18F]fluororasagiline, a novel positron emission tomography (PET) radioligand for monoamine oxidase B (MAO-B). *Bioorg. Med. Chem.* 20, 3065–3071. doi: 10.1016/j.bmc.2012.02.056
- Nag, S., Varrone, A., Toth, M., Thiele, A., Ketschau, G., Heinrich, T., et al. (2012b). In vivo evaluation in cynomolgus monkey brain and metabolism of [18F]fluorodeprenyl: a new MAO-B pet radioligand. *Synapse* 66, 323–330. doi: 10.1002/syn.21514
- Nag, S., Lehmann, L., Ketschau, G., Toth, M., Heinrich, T., Thiele, A., et al. (2013). Development of a novel fluorine-18 labeled deuterated fluororasagiline (([18F]fluororasagiline-D2) radioligand for PET studies of monoamine oxidase B (MAO-B). *Bioorg. Med. Chem.* 21, 6634–6641. doi: 10.1016/j.bmc.2013.08.019
- Narayanaswami, V., Drake, L. R., Brooks, A. F., Meyer, J. H., Houle, S., Kilbourn, M. R., et al. (2019). Classics in neuroimaging: development of PET tracers for imaging monoamine oxidases. *ACS Chem. Neurosci.* 10, 1867–1871. doi: 10.1021/acscchemneuro.9b00081
- Narayanaswami, V., Tong, J., Schifani, C., Bloomfield, P. M., Dahl, K., and Vasdev, N. (2021). Preclinical evaluation of TSPO and MAO-B PET radiotracers in an LPS model of neuroinflammation. *PET Clin.* 16, 233–247. doi: 10.1016/j.cpet.2020.12.003
- Ng, K. P., Pascoal, T. A., Mathotaarachchi, S., Therriault, J., Kang, M. S., Shin, M., et al. (2017). Monoamine oxidase B inhibitor, selegiline, reduces ¹⁸F-THK5351 uptake in the human brain. *Alzheimers Res. Ther.* 9:25. doi: 10.1186/s13195-017-0253-y
- Ng, K. P., Therriault, J., Kang, M. S., Struyfs, H., Pascoal, T. A., Mathotaarachchi, S., et al. (2019). Rasagiline, a monoamine oxidase B inhibitor, reduces in vivo [18F]THK5351 uptake in progressive supranuclear palsy. *Neuroimage Clin.* 24:102091. doi: 10.1016/j.nicl.2019.102091
- Ni, R., Rojdnier, J., Voytenko, L., Dyrks, T., Thiele, A., Marutle, A., et al. (2021). In vitro characterization of the regional binding distribution of amyloid PET tracer florbetaben and the glia tracers deprenyl and PK11195 in autopsy Alzheimer's brain tissue. *J. Alzheimers Dis.* 80, 1723–1737. doi: 10.3233/JAD-201344
- Nordberg, A., Carter, S. F., Rinne, J., Drzezga, A., Brooks, D. J., Vandenberghe, R., et al. (2013). A European multicentre PET study of fibrillar amyloid in Alzheimer's disease. *Eur. J. Nucl. Med. Mol. Imaging* 40, 104–114. doi: 10.1007/s00259-012-2237-2
- Okamura, N., Harada, R., Ishiki, A., Kikuchi, A., Nakamura, T., and Kudo, Y. (2018). The development and validation of tau PET tracers: current status and future directions. *Clin. Transl. Imaging* 6, 305–316. doi: 10.1007/s40336-018-0290-y
- Olmos, G., Alemany, R., Boronat, M. A., and Garcia-Sevilla, J. A. (1999). Pharmacologic and molecular discrimination of 12-imidazoline receptor subtypes. *Ann. N. Y. Acad. Sci.* 881, 144–160. doi: 10.1111/j.1749-6632.1999.tb09354.x
- Olmos, G., Alemany, R., Escriba, P. V., and Garcia-Sevilla, J. A. (1994). The effects of chronic imidazoline drug treatment on glial fibrillary acidic protein concentrations in rat brain. *Br. J. Pharmacol.* 111, 997–1002. doi: 10.1111/j.1476-5381.1994.tb14842.x
- Olsen, M., Aguilar, X., Sehlin, D., Fang, X. T., Antoni, G., Erlandsson, A., et al. (2018). Astroglial responses to amyloid-beta progression in a mouse model of Alzheimer's disease. *Mol. Imaging Biol.* 20, 605–614. doi: 10.1007/s11307-017-1153-z
- Ory, D., Planas, A., Dresselaers, T., Gsell, W., Postnov, A., Celen, S., et al. (2015). PET imaging of TSPO in a rat model of local neuroinflammation induced by intracerebral injection of lipopolysaccharide. *Nucl. Med. Biol.* 42, 753–761. doi: 10.1016/j.nucmedbio.2015.06.010
- Parini, A., Moudanos, C. G., Pizzinat, N., and Lanier, S. M. (1996). The elusive family of imidazoline binding sites. *Trends Pharmacol. Sci.* 17, 13–16. doi: 10.1016/0165-6147(96)81564-1
- Park, S., Oh, M., Kim, J. S., Lee, J. H., Yoon, Y. W., and Roh, J. H. (2021). ¹⁸F-THK-5351, Fluorodeoxyglucose, and Florbetaben PET images in atypical Alzheimer's disease: a pictorial insight into disease pathophysiology. *Brain Sci.* 11:465. doi: 10.3390/brainsci11040465
- Parker, C. A., Nabulsi, N., Holden, D., Lin, S. F., Cass, T., Labaree, D., et al. (2014). Evaluation of 11C-BU99008, a PET ligand for the imidazoline2 binding sites in rhesus brain. *J. Nucl. Med.* 55, 838–844. doi: 10.2967/jnumed.113.131854
- Pekny, M., Pekna, M., Messing, A., Steinhauser, C., Lee, J. M., Parpura, V., et al. (2016). Astrocytes: a central element in neurological diseases. *Acta Neuropathol.* 131, 323–345. doi: 10.1007/s00401-015-1513-1
- Ramsden, M., Kotilinek, L., Forster, C., Paulson, J., McGowan, E., Santacruz, K., et al. (2005). Age-dependent neurofibrillary tangle formation, neuron loss, and memory impairment in a mouse model of human tauopathy (P301L). *J. Neurosci.* 25, 10637–10647. doi: 10.1523/JNEUROSCI.3279-05.2005
- Regunathan, S., Feinstein, D. L., and Reis, D. J. (1993). Expression of non-adrenergic imidazoline sites in rat cerebral cortical astrocytes. *J. Neurosci. Res.* 34, 681–688.

- Remaury, A., Raddatz, R., Ordener, C., Savic, S., Shih, J. C., Chen, K., et al. (2000). Analysis of the pharmacological and molecular heterogeneity of I(2)-imidazoline-binding proteins using monoamine oxidase-deficient mouse models. *Mol. Pharmacol.* 58, 1085–1090. doi: 10.1124/mol.58.5.1085
- Rodriguez-Vieitez, E., Ni, R., Gulyas, B., Toth, M., Haggkvist, J., Halldin, C., et al. (2015). Astrocytosis precedes amyloid plaque deposition in Alzheimer APPswe transgenic mouse brain: a correlative positron emission tomography and in vitro imaging study. *Eur. J. Nucl. Med. Mol. Imaging* 42, 1119–1132. doi: 10.1007/s00259-015-3047-0
- Rodriguez-Vieitez, E., Saint-Aubert, L., Carter, S. F., Almkvist, O., Farid, K., Scholl, M., et al. (2016). Diverging longitudinal changes in astrocytosis and amyloid PET in autosomal dominant Alzheimer's disease. *Brain* 139, 922–936.
- Ruiz, J., Martin, I., Callado, L. F., Meana, J. J., Barturen, F., and Garcia-Sevilla, J. A. (1993). Non-adrenoceptor [3H]idazoxan binding sites (I2-imidazoline sites) are increased in postmortem brain from patients with Alzheimer's disease. *Neurosci. Lett.* 160, 109–112. doi: 10.1016/0304-3940(93)90925-b
- Rusjan, P. M., Wilson, A. A., Miler, L., Fan, L., Mizrahi, R., Houle, S., et al. (2014). Kinetic modeling of the monoamine oxidase B radioligand [¹¹C]SL25.1188 in human brain with high-resolution positron emission tomography. *J. Cereb. Blood Flow Metab.* 34, 883–889. doi: 10.1038/jcbfm.2014.34
- Saba, W., Valette, H., Peyronneau, M. A., Bramouille, Y., Coulon, C., Curet, O., et al. (2010). [(11C)SL25.1188, a new reversible radioligand to study the monoamine oxidase type B with PET: preclinical characterisation in nonhuman primate. *Synapse* 64, 61–69. doi: 10.1002/syn.20703
- Saito, T., Matsuba, Y., Mihira, N., Takano, J., Nilsson, P., Itohara, S., et al. (2014). Single App knock-in mouse models of Alzheimer's disease. *Nat. Neurosci.* 17, 661–663.
- Saitoh, Y., Imabayashi, E., Mukai, T., Matsuda, H., and Takahashi, Y. (2021). Visualization of motor cortex involvement by 18F-THK5351 PET potentially strengthens diagnosis of amyotrophic lateral sclerosis. *Clin. Nucl. Med.* 46, 243–245. doi: 10.1097/RLU.00000000000003456
- Santillo, A. F., Gambini, J. P., Lannfelt, L., Langstrom, B., Ulla-Marja, L., Kilander, L., et al. (2011). In vivo imaging of astrocytosis in Alzheimer's disease: an ¹¹C-L-deuteriodesprenyl and PIB PET study. *Eur. J. Nucl. Med. Mol. Imaging* 38, 2202–2208. doi: 10.1007/s00259-011-1895-9
- Sastre, M., and Garcia-Sevilla, J. A. (1993). Opposite age-dependent changes of alpha 2A-adrenoceptors and nonadrenoceptor [3H]idazoxan binding sites (I2-imidazoline sites) in the human brain: strong correlation of I2 with monoamine oxidase-B sites. *J. Neurochem.* 61, 881–889. doi: 10.1111/j.1471-4159.1993.tb03599.x
- Saura, J., Kettler, R., Da Prada, M., and Richards, J. G. (1992). Quantitative enzyme radioautography with 3H-Ro 41-1049 and 3H-Ro 19-6327 in vitro: localization and abundance of MAO-A and MAO-B in rat CNS, peripheral organs, and human brain. *J. Neurosci.* 12, 1977–1999. doi: 10.1523/JNEUROSCI.12-05-01977.1992
- Saura, J., Luque, J. M., Cesura, A. M., Da Prada, M., Chan-Palay, V., Huber, G., et al. (1994). Increased monoamine oxidase B activity in plaque-associated astrocytes of Alzheimer brains revealed by quantitative enzyme radioautography. *Neuroscience* 62, 15–30. doi: 10.1016/0306-4522(94)90311-5
- Schaefferbeke, J., Evenepoel, C., Declercq, L., Gabel, S., Meersmans, K., Bruffaerts, R., et al. (2018). Distinct [¹⁸F]THK5351 binding patterns in primary progressive aphasia variants. *Eur. J. Nucl. Med. Mol. Imaging* 45, 2342–2357. doi: 10.1007/s00259-018-4075-3
- Scholl, M., Carter, S. F., Westman, E., Rodriguez-Vieitez, E., Almkvist, O., Thordardottir, S., et al. (2015). Early astrocytosis in autosomal dominant Alzheimer's disease measured in vivo by multi-tracer positron emission tomography. *Sci. Rep.* 5:16404. doi: 10.1038/srep16404
- Schonecker, S., Brendel, M., Palleis, C., Beyer, L., Hoglinger, G. U., Schuh, E., et al. (2019). PET Imaging of Astrogliosis and Tau Facilitates Diagnosis of Parkinsonian Syndromes. *Front Aging Neurosci.* 11:249. doi: 10.3389/fnagi.2019.00249
- Shimizu, S., Imabayashi, E., Takenoshita, N., Okamura, N., Furumoto, S., Kudo, Y., et al. (2018). Case of progressive supranuclear palsy detected by tau imaging with [¹⁸F]THK-5351 before the appearance of characteristic clinical features. *Geriatr. Gerontol. Int.* 18, 501–502. doi: 10.1111/ggi.13229
- Son, H. J., Oh, J. S., Roh, J. H., Seo, S. W., Oh, M., Lee, S. J., et al. (2019). Differences in gray and white matter ¹⁸F-THK5351 uptake between behavioral-variant frontotemporal dementia and other dementias. *Eur. J. Nucl. Med. Mol. Imaging* 46, 357–366. doi: 10.1007/s00259-018-4125-x
- Sur, C., Zeng, Z., Hostetler, E., Connolly, B. M., Miller, P. J., O'malley, S., et al. (2010). In vitro Characterization of MK-3328: a novel fluorinated positron emission tomography tracer for plaques. *Alzheimers Dement.* 6:S40. doi: 10.1016/j.jalz.2010.05.112
- Tago, T., Furumoto, S., Okamura, N., Harada, R., Adachi, H., Ishikawa, Y., et al. (2016). Structure-activity relationship of 2-Arylquinolines as PET imaging tracers for tau pathology in Alzheimer disease. *J. Nucl. Med.* 57, 608–614. doi: 10.2967/jnumed.115.166652
- Tago, T., Toyohara, J., Sengoku, R., Murayama, S., and Ishii, K. (2019). Monoamine oxidase B binding of 18F-THK5351 to visualize glioblastoma and associated gliosis: an autopsy-confirmed case. *Clin. Nucl. Med.* 44, 507–509. doi: 10.1097/RLU.00000000000002564
- Takaya, M., Ishii, K., Hosokawa, C., Saigoh, K., and Shirakawa, O. (2018). Tau accumulation in two patients with frontotemporal lobe degeneration showing different types of aphasia using 18F-THK-5351 positron emission tomography: a case report. *Int. Psychogeriatr.* 30, 641–646. doi: 10.1017/S1041610217002277
- Tesson, F., Limon-Boulez, I., Urban, P., Puype, M., Vandekerckhove, J., Couprie, I., et al. (1995). Localization of I2-imidazoline binding sites on monoamine oxidases. *J. Biol. Chem.* 270, 9856–9861. doi: 10.1074/jbc.270.17.9856
- Tesson, F., Prip-Buus, C., Lemoine, A., Pegorier, J. P., and Parini, A. (1991). Subcellular distribution of imidazoline-guanidinium-receptive sites in human and rabbit liver. Major localization to the mitochondrial outer membrane. *J. Biol. Chem.* 266, 155–160. doi: 10.1016/s0021-9258(18)52415-7
- Tong, J., Meyer, J. H., Furukawa, Y., Boileau, I., Chang, L. J., Wilson, A. A., et al. (2013). Distribution of monoamine oxidase proteins in human brain: implications for brain imaging studies. *J. Cereb. Blood Flow Metab.* 33, 863–871. doi: 10.1038/jcbfm.2013.19
- Tong, J., Rathitharan, G., Meyer, J. H., Furukawa, Y., Ang, L. C., Boileau, I., et al. (2017). Brain monoamine oxidase B and A in human Parkinsonian dopamine deficiency disorders. *Brain* 140, 2460–2474. doi: 10.1093/brain/awx172
- Tyacke, R. J., Fisher, A., Robinson, E. S., Grundt, P., Turner, E. M., Husbands, S. M., et al. (2012). Evaluation and initial in vitro and ex vivo characterization of the potential positron emission tomography ligand, BU99008 (2-(4,5-dihydro-1H-imidazol-2-yl)-1-methyl-1H-indole), for the imidazoline(2) binding site. *Synapse* 66, 542–551. doi: 10.1002/syn.21541
- Tyacke, R. J., Myers, J. F. M., Venkataraman, A., Mick, I., Turton, S., Passchier, J., et al. (2018). Evaluation of ¹¹C-BU99008, a PET ligand for the imidazoline₂ binding site in human brain. *J. Nucl. Med.* 59, 1597–1602. doi: 10.2967/jnumed.118.208009
- Uchida, Y., Horimoto, Y., Shibata, H., Kuno, T., Usami, T., Takada, K., et al. (2021). Occipital tau deposition and astrogliosis after traumatic brain injuries in a kendo player. *Neurol. Clin. Pract.* 11, e579–e581. doi: 10.1212/CPJ.0000000000000936
- Venkataraman, A. V., Keat, N., Myers, J. F., Turton, S., Mick, I., Gunn, R. N., et al. (2018). First evaluation of PET-based human biodistribution and radiation dosimetry of ¹¹C-BU99008, a tracer for imaging the imidazoline₂ binding site. *EJNMMI Res.* 8:71. doi: 10.1186/s13550-018-0429-x
- Verberk, I. M. W., Thijssen, E., Koelewijn, J., Mauroo, K., Vanbrabant, J., De Wilde, A., et al. (2020). Combination of plasma amyloid beta(1-42/1-40) and glial fibrillary acidic protein strongly associates with cerebral amyloid pathology. *Alzheimers Res. Ther.* 12:118. doi: 10.1186/s13195-020-00682-7
- Vermeiren, C., Motte, P., Viot, D., Mairet-Coello, G., Courade, J. P., Citron, M., et al. (2018). The tau positron-emission tomography tracer AV-1451 binds with similar affinities to tau fibrils and monoamine oxidases. *Mov. Disord.* 33, 273–281. doi: 10.1002/mds.27271
- Villemagne, V. L., Harada, R., Dore, V., Furumoto, S., Mulligan, R. S., Kudo, Y., et al. (2022). Assessing reactive astrogliosis with ¹⁸F-SMBT-1 across the Alzheimer's disease spectrum. *J. Nucl. Med.* jnumed.121.263255. doi: 10.2967/jnumed.121.263255

- Wilson, H., Dervenoulas, G., Pagano, G., Tyacke, R. J., Polychronis, S., Myers, J., et al. (2019). Imidazoline 2 binding sites reflecting astroglia pathology in Parkinson's disease: an in vivo ^{11}C -BU99008 PET study. *Brain* 142, 3116–3128. doi: 10.1093/brain/awz260
- Yoshimoto, M., Hirata, M., Kagawa, S., Magata, Y., Ohmomo, Y., and Temma, T. (2019). Synthesis and characterization of novel radiofluorinated probes for positron emission tomography imaging of monoamine oxidase B. *J. Labelled Comp. Radiopharm.* 62, 580–587. doi: 10.1002/jlcr.3779
- Youdim, M. B., Edmondson, D., and Tipton, K. F. (2006). The therapeutic potential of monoamine oxidase inhibitors. *Nat. Rev. Neurosci.* 7, 295–309.
- Zhang, L., Hu, K., Shao, T., Hou, L., Zhang, S., Ye, W., et al. (2021). Recent developments on PET radiotracers for TSPO and their applications in neuroimaging. *Acta Pharm. Sin. B* 11, 373–393. doi: 10.1016/j.apsb.2020.08.006

Conflict of Interest: NO and YK hold stocks in CLINO Co., Ltd. RH, SF, and NO were scientific consultants for CLINO Co., Ltd.

The authors declare that this study received funding from Clino Ltd. The funder was not involved in the study design, collection, analysis, interpretation of data, the writing of this article, or the decision to submit it for publication.

Publisher's Note: All claims expressed in this article are solely those of the authors and do not necessarily represent those of their affiliated organizations, or those of the publisher, the editors and the reviewers. Any product that may be evaluated in this article, or claim that may be made by its manufacturer, is not guaranteed or endorsed by the publisher.

Copyright © 2022 Harada, Furumoto, Kudo, Yanai, Villemagne and Okamura. This is an open-access article distributed under the terms of the Creative Commons Attribution License (CC BY). The use, distribution or reproduction in other forums is permitted, provided the original author(s) and the copyright owner(s) are credited and that the original publication in this journal is cited, in accordance with accepted academic practice. No use, distribution or reproduction is permitted which does not comply with these terms.